Vol. 256: 1–11, 2003 | MARINE ECOLOGY PROGRESS SERIES
Mar Ecol Prog Ser | Published July 17

UV (280 to 400 nm) optical properties in a Norwegian fjord system and an intercomparison of underwater radiometers

Berit Kjeldstad[1,*], Øyvind Frette[2], Svein Rune Erga[3], Howard I. Browman[4], Penny Kuhn[5], Richard Davis[5], William Miller[5], Jakob J. Stamnes[2]

[1]Department of Physics, Norwegian University of Science and Technology, 7491 Trondheim, Norway
[2]Department of Physics, and [3]Department of Microbiology, University of Bergen, 5020 Bergen, Norway
[4]Institute of Marine Research, Austevoll Aquaculture Research Station, 5392 Storebø, Norway
[5]Department of Oceanography, Dalhousie University, Halifax B3H 4J1, Canada

ABSTRACT: The depth to which solar ultraviolet (UV) radiation penetrates water columns is highly variable. The range in diffuse attenuation coefficients observed in the clearest ocean waters versus small oligotrophic lakes can be as much as 3 orders of magnitude. In this study, we investigated the variability of UV penetration (and its sources) in a typical Norwegian fjord system (Samnanger fjord, 60° N, 5° E) after the main spring diatom bloom had passed, so that the primary production in the fjord was low, with chl *a* concentrations of 1 to 2 mg m^{-3} at 10 m depth (April 1999). At 320 nm, diffuse attenuation coefficients varied between 1.2 and 5.0 m^{-1} from the outer to the inner part of the fjord. At 305 nm, the variation was between 2.3 and 5.4 m^{-1}. Less variability was found at longer wavelengths (340 and 380 nm). River run off, containing high concentrations of colored dissolved organic matter (CDOM), provided a low salinity layer of highly UV-absorbing water at the surface. There was a strong correlation between diffuse attenuation coefficients in the UV and CDOM, but only a weak correlation with chl *a*. Uncertainty in measuring diffuse attenuation coefficients are seldom addressed. Thus, we undertook an intercomparison of diffuse attenuation coefficients calculated from data produced using 3 different UV radiometers: a spectroradiometer, a narrowband filter radiometer and 2 moderate-bandwidth filter radiometers. The deviations in attenuation ranged from 20 to 40%, being most pronounced at the shortest wavelengths (305 and 320 nm) at 3 different stations. This intercomparison illustrates that there has not been significant improvement in the uncertainties of measuring diffuse attenuation coefficients since a similar intercomparison was performed in 1994.

KEY WORDS: Ultraviolet radiation · Fjord · Marine · Penetration · Attenuation · Intercomparison

INTRODUCTION

Ultraviolet radiation (UV; 280 to 400 nm) is an important environmental regulating factor for life in water (e.g. De Mora et al. 2000, Hessen 2001). Since marine phytoplankton are the basic components in the earth's largest ecosystem, even small reductions in photosynthetic rates associated with increased UVB (280 to 320 nm) radiation could negatively affect higher trophic levels (Browman et al. 2000). Thus, knowledge of UV penetration into different water types is central to evaluations of the biological and ecological impacts of UV radiation.

The depth to which UV penetrates fresh and marine waters is highly variable. The range in diffuse attenuation coefficients from the clearest ocean waters to small turbid lakes can be as much as 3 orders of magnitude (Booth et al. 1997, Kuhn et al. 1999, Gunn et al. 2001). Published investigations of freshwater habitats, ranging from temperate lakes (Scully & Lean 1994) and wetland waters (Arts et al. 2000) to small ponds (Crump et al. 1999), demonstrate an extremely broad

*Email: berit.kjeldstad@phys.ntnu.no

range of optical characteristics. Although there appears to be less variability in marine systems, there are considerable differences between transparent oceanic water found in the Antarctic (Neale et al. 1998), Arctic (Aas & Høkedal 1996), tropical (Dunne & Brown 1996) and North European coastal regions (Aas & Højerslev 2001), and more turbid water in coastal lagoons with strong attenuation of UV radiation (Piazena & Häder 1994, Conde et al. 2000).

For Norwegian fjords, knowledge of UV penetration is scarce or lacking. However, data exist from the Oslo fjord and the Hardanger fjord from the early 1970s (Aas & Højerslev 2001). Due to complex exchange processes between coastal water and fjord water, the optical properties of fjord water may be of great importance both because of their direct effects within the fjord ecosystem itself, and because of their influence on optical properties in the more extensive, adjacent coastal ecosystem.

Measuring UV radiation is challenging and consequently requires careful attention to instrument performance. The absolute accuracy of spectral global irradiance values made with different instruments can vary by 20% or more (Kjeldstad et al. 1997, Webb 1997). Proper correction for different instrument response characteristics, which are the source of some of these discrepancies, can reduce deviations to 2–3% (Bais et al. 2001). Since 1990, repeated intercomparisons of terrestrial instruments has improved results (Bais et al. 2001). A similar process has not as yet been undertaken for underwater-measurement instruments. Comparisons of instruments with very different bandwidths and light collection characteristics are complicated (Leszczynski et al. 1998). Underwater UV measurements are even more challenging than terrestrial measurements, and this can result in a high level of uncertainty associated with many investigations of UV penetration in water. Kirk et al. (1994) compared UV measurements using spectroradiometers and moderate-bandwidth filter instruments at different depths in 2 lakes, and found differences of at least the same magnitude as those for terrestrial measurements. For some instruments, even larger discrepancies were found. Diffuse attenuation coefficients were compared in both colorless and weakly colored water — deviations between instruments of up to 20% were reported (Kirk et al. 1994). To the best of our knowledge, this is the only published intercomparison of diffuse attenuation coefficients obtained simultaneously from different underwater UV radiometers at a single site.

The aim of this study was to (1) survey the variability of UV penetration in a typical western Norwegian fjord, (2) investigate the water quality variables that control UV penetration, and (3) perform an intercomparison of UV radiometers. Measurements were made just after the end of the spring diatom bloom. Therefore, the primary production of the fjord was low, with phytoplankton cells generally confined to the upper 25 m of the water column. Several different UV-optimized instruments were deployed during this survey, allowing us to compare irradiance profiles and diffuse attenuation coefficients derived from 3 different commonly used UV radiometers. The intercomparison campaign was performed at 4 selected stations in the fjord characterized by different UV transparencies.

MATERIALS AND METHODS

Study site. The investigations were carried out at 4 fixed stations along a transect in the Samnanger fjord, western Norway, in late April (26 to 30) 1999. The stations were located at 60° 23′ N, 05° 44′ E (Stn 1), 60° 18′ N, 05° 38′ E (Stn 3), 60° 13′ N, 05° 38′ E (Stn 5),

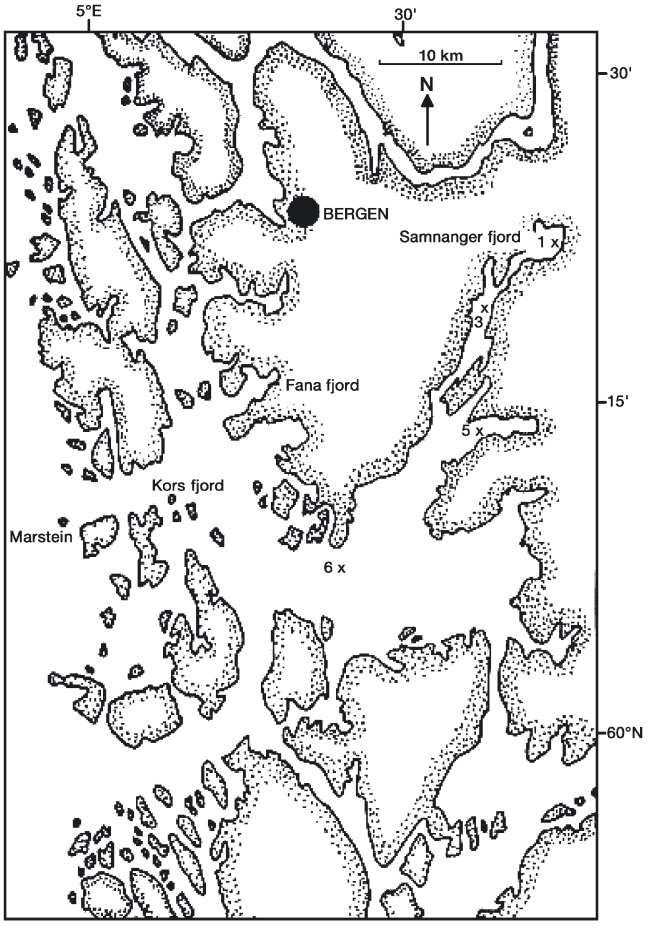

Fig. 1. Location of Stns 1, 3, 5, and 6 in the Samnanger fjord, Norway. Profiling measurements were carried out on one cruise from 26 to 30 April 1999. Stn 1: 60° 23′ N, 05° 44′ E (depth 239 m), Stn 3: 60° 18′ N, 05° 38′ E (depth 238 m), Stn 5: 60° 13′ N, 05° 38′ E (depth 253 m), Stn 6: 60° 07′ N, 05° 26′ E (depth 603 m)

and 60° 07′ N, 05° 26′ E (Stn 6) (Fig. 1). The RV 'Hans Brattstrøm', belonging to the University of Bergen, was used for the field work. It is well suited for performing underwater light measurements because it is relatively small (24 m long) and equipped with a long armed crane on the aft deck for deployment of instruments up to 4 m away from the vessel. Therefore, the measurements were not strongly biased by the presence of the vessel. UV penetration was measured at Stns 1, 3, 5 and 6 (Fig. 1) on each of 3 consecutive days (26 to 28 April) in order to map the spatial variability in UV transmittance within this typical Norwegian fjord. Measurements were made using several spectroradiometers, allowing for an intercomparison of results. On one day (29 April 1999), a comprehensive investigation of hydrography, colored dissolved organic matter (CDOM), and phytoplankton species composition and biomass was undertaken at 3 of the stations (Stns 1, 3 and 5) in addition to UV penetration measurements. On this date, only one of the radiometers was used because time was limited. Water depth was 240 to 250 m at all stations.

Chl *a*. Samples of chl *a* were filtered onto Whatman GF/F filters and stored frozen until analyses were done a few weeks later. Chl *a* was analyzed fluorimetrically (Turner Designs-10) with 90% acetone as solvent (Holm-Hansen et al. 1965).

Temperature and salinity. Temperature and salinity profiles were obtained using a calibrated Sea Bird 911 CTD deployed with a winch.

CDOM. Measurements of CDOM were made using the methods described by Højerslev & Aas (1998). Water samples were filtered through a 0.2 µm Nucleopore filter, and stored in opaque glass bottles at 4°C until analyses were performed a few weeks later. We assumed that the filtered water was dominated optically by yellow substance, although particles less than the pore size of the filter may influence the results (Aas pers. com.). In the laboratory, the spectral absorptance of the water samples (250 to 650 nm) was measured using a 10 cm quartz cuvette in a Shimadzu MPS 2000 spectrometer. In the curve fitting required to determine the absorption coefficient at 310 nm, only data in the 275 to 425 nm waveband were used (as recommended by Højerslev & Aas 1998). The absorption coefficient at 310 nm, a_y, was used as a measure of CDOM.

Description of optical instruments deployed. ***Absorption and attenuation coefficient measurements:*** Profiles of absorption and attenuation coefficients were measured directly using an ac9 instrument (Wet Labs) deployed using a winch. Water was pumped through the detector tube. Both absorption and attenuation could be measured simultaneously at 9 different wavelengths between 410 and 715 nm. Only data from the 410 nm channels are reported here.

Downwelling spectral irradiance measurements: The spectroradiometer used was an OL754-O-PMT (Optronic Laboratories; abbreviation: OL754) outfitted with a 16 m long quartz optical fiber and a submersible 100 mm diameter integrating sphere. This spectroradiometer is a double monochromator optimized for UV with a full-width-half-maximum (FWHM) of 1 nm. The instrument was calibrated and operated according to procedures described in Kuhn et al. (1999). The underwater sensor was deployed approximately 1 m from the research ship at the stern. Vertical profiles of diffuse downwelling attenuation coefficients (K_d) were calculated from scans taken between 290 and 400 nm at 1 nm intervals and at 3 depths, between 0 and 1 m, 1 and 2 m, and 2 and 3 m. The scans were taken under stable cloud conditions with as little variation in the direct beam as possible during the measurements at each station. K_d was calculated from these data as logarithmic ratios between downwelling irradiances at different depths (see Kuhn et al. 1999).

Narrowband filter radiometer: A narrowband filter radiometer (SeaWifs Multichannel Profiling Radiometer [SMPR], Satlantic) measured UV radiation at 4 channels (305, 323, 338, and 380 nm) in addition to visible radiation at several channels. The FWHM was between 2 and 10 nm for each channel. Both a profiling and a surface SMPR unit were used. The profiling unit was a freefalling instrument that measured downwelling irradiance at different depths, $E_d(z)$, and the floating surface unit measured the downwelling irradiance just below the surface, $E_{d,s}$. The measurement frequency was 6 Hz. The instrument was operated from the rear of the ship, and launched several meters from the ship to minimize effects of ship shadows.

K_d values were calculated from logarithmic ratios between downwelling irradiances recursively. After the first fit, residuals were calculated. From these and the root mean square error, 4 test vectors were generated: (1) internal studentized residuals, (2) external studentized residuals, (3) Cook's D statistic, and (4) Atkinson's T statistic. Any data point whose residuals produced test values that all were greater than twice the standard deviation of the whole data set was considered as an outlier and rejected. The remaining data were then fitted again. This recursive process was repeated until no more outliers were generated.

Moderate-bandwidth filter radiometer: Two identical moderate-bandwidth filter radiometers PUV 500 (Biospherical instruments; abbreviation: PUV500) were used to measure UV at 4 channels with center wavelengths at 305, 320, 340, and 380 nm. The FWHM was 10 nm for all channels, except for the 305 nm channel, which had a short-cut filter, cutting radiation above 310 nm. Thus, the effective center wavelength of the

305 nm channel depended on the spectral distribution of the solar irradiance, as discussed by Booth et al. (1994). With high attenuation of UV as was the case in Samnanger fjord, 308 nm was found to be the efficient spectral wavelength with which to compare the 305 nm channel (see Figs. 5 & 6). Both underwater units were used together with the same surface unit (PUV 510, Biospherical instruments). The measurement frequency was 1 Hz for all 3 units. Measurements were performed at that side of the ship which faced the sun. The surface unit was situated on the upper deck. Both underwater units were kept in water 15 min prior to measurements in order to stabilize the temperature of the detectors. This is most important for the 305 nm channel, which has a slower response to temperature stabilization than the other channels. Measurements were adjusted for dark current, which is extremely important for the shorter wavelengths at low intensities. K_d values were calculated as logarithmic ratios between downwelling irradiance. The irradiance data had been fitted to a linear regression. The depth sensors of both instruments were compared with a high resolution Simrad EQ55 Echo Sounder and adjusted for any bias.

Measurement protocol for UV transmittance variability: The 1 d transect conducted on 29 April 1999 covered 3 stations starting from the most easterly (inner) part of the fjord at Stn 1 and proceeding southwest to Stn 3 and finally to Stn 5. At each station, the whole sequence of optical measurements and water quality investigations were completed within 2 h. During the measurements at each station, the boat was kept in the same position. The wind conditions were the same at all stations, with wind speeds less than 5 m s^{-1}. The solar zenith angles were 51°, 50°, and 64° at Stns 1, 3, and 5, respectively, when irradiance profiles were performed. The maximum total irradiance at solar noon (at a solar zenith angle of 46°) was 800 W m^{-2} measured with an Eppley pyranometer. The PUV500 and the ac9 were launched immediately after each other at each station. Water samples of chl *a* and yellow substance were taken just before the optical measurements. Only one UV profiling instrument (PUV500/510) was used during this transect due to lack of time.

Measurement protocol for comparing diffuse attenuation coefficients at different locations: To compare diffuse attenuation coefficients (at the same location) calculated from the data of the different instruments, we measured downwelling irradiances with several radiometers at each station. Only one radiometer could be lowered into the water at a time, prohibiting simultaneous measurements. However, at each station, measurements with all instruments were conducted within 1 to 2 h, minimizing changes in solar elevation and keeping both the direct and the diffuse radiation as constant as possible during the deployment of all instruments. Profiles were taken at Stn 1 on 27 April under clear sky conditions with no wind and solar zenith angles between 54° and 60°. Measurements at Stn 3 were also performed on 27 April at solar zenith angles between 46° and 53°. On 28 April, profiles were taken at Stn 5 under slightly changing cloud conditions at solar zenith angles between 46° and 54°. Finally, measurements at Stn 6 were performed on 30 April under windy, rainy, and overcast conditions. There were swells of 0.5 m, and the solar zenith angle varied between 48° and 56°. It was possible to perform intercomparisons of diffuse attenuation coefficients in different water types and under different weather conditions at all 4 stations. Spectral measurements with OL754 were performed at 3 depths (if possible), just below the surface (0 m), at 1 and 2 m. At each depth, a 290 to 400 nm spectral scan was conducted at 1 nm intervals. The filter radiometer instruments performed profiling at a high sampling frequency at all channels, as described above. Simultaneous measurements with the surface units allowed for corrections for variable clouds during the profiling.

RESULTS

The Samnanger fjord, south of Bergen, Norway, is connected with the coastal water at the outer (western) part. The inner (eastern) part of the fjord receives water from rivers. In such a system, the water quality is highly variable in time and space.

Variability in UV penetration in the fjord

The 1 d transect was conducted after the first decline of the spring bloom and revealed the variability in UV penetration from one station to another within a limited time interval. Chlorophyll concentrations were low, ranging from 0.7 to 1.8 mg m^{-3} in the upper 10 m layer (Table 1) with the highest concentrations between 1.4 and 1.8 mg m^{-3} at Stn 5, closest to the coast. The salinity never exceeded 30 ppt above 10 m depth at any station. Only the upper 10 m layer of the water column was investigated, since no UV radiation was detectable at lower depths. At the innermost location (Stn 1) there was a freshwater surface layer that extended down to about 1 m. It had a salinity as low as 6.9 ppt just below the surface that increased to 27.7 ppt at 2 m (Table 1). A freshwater surface layer was also present at Stns 3 and 5, but significantly less pronounced than at Stn 1.

Table 1. Chl *a*, colored dissolved organic matter (CDOM; measured as absorption at 310 nm), absorption and attenuation at 410 nm measured with an ac9 profiling instrument, diffuse attenuation coefficients calculated from downwards irradiance 305, 320, 340 and 380 nm measured with PUV, salinity and temperature at different depths intervals at stations sampled in Samnanger Fjord, Norway (see 'Materials and methods' for more details) K_{d305nm}, K_{d320nm}, K_{d340nm}, and K_{d380nm} retrieved from downwards irradiance from moderate bandwidth filter radiometer (PUV500) at given depth intervals. Empty rubrics, data not available. a_{410nm} and c_{410nm}: absorption and attenuation at 410 nm, respectively, measured with an ac9 profiling instrument. K_{d305nm}, K_{d320nm}, K_{d340nm} and K_{d380nm}: diffuse attenuation coefficients calculated from downwards irradiance 305, 320, 340 and 380 nm, respectively

Stn	Physical depth (m)	Chl *a* (mg m^{-3})	CDOM a_{y310nm} (m^{-1})	a_{410nm} (m^{-1})	c_{410nm} (m^{-1})	K_{d305nm} (m^{-1})	K_{d320nm} (m^{-1})	K_{d340nm} (m^{-1})	K_{d380nm} (m^{-1})	Salinity (ppt)	Temp. (°C)
1	0[a]–1	0.78	3.22	1.31	1.55	5.4	5.0	3.8	2.3	6.9	6.4
	1–2						2.0	1.5	0.9	27.7	8.0
	7–10[a]	1.01	1.04	0.50	0.87				0.78	30.0	6.3
3	0[a]–1	0.91	2.11	0.65	1.01	3.24	2.37	1.74	1.01	23.3	9.2
	1–2						2.11	1.54	0.86	26.0	8.6
	7–10[a]	0.73	1.52	0.47	0.68				0.63	29.7	6.3
5	0[a]–1	1.37	1.82	0.57	1.1	2.30	1.90	1.36	0.76	26.8	9.3
	1–2						1.82	1.31	0.72	27.9	8.8
	7–10[a]	1.81	1.67	0.50	0.80				0.65	29.5	6.4

[a]Depth at which chl *a*, CDOM, a_{410nm}, c_{410nm}, salinity and temperature were measured

The most important parameter governing the inherent optical properties of the Samnanger fjord after the decline of the spring bloom is the concentration of CDOM. The absorption coefficient at 410 nm (denoted by a_{410nm} in Table 1) was correlated with the concentration of CDOM, which was measured indirectly by the absorption at 310 nm in water samples collected at 2 depths, as described in 'Materials and methods'. At all 3 stations a larger absorption was found near the surface (0 to 1 m) than at greater depths (7 to 10 m) (although this is most pronounced at Stn 1). Profiles of the absorption at 410 nm were taken as well (the complete data set is not shown in Table 1). They revealed a pattern similar to that for CDOM, i.e. a larger absorption in the surface layer (0 to 1 m) than at greater depths (below 3 m). Correlation analyses between CDOM and a_{410nm} gave a high correlation (r = 0.93) (Fig. 2a). The correlation between a_{410nm} and the chl *a* concentration was poor (r = –0.04) (Fig. 2b), clearly showing that CDOM dominates the absorption at 410 nm in these water layers.

UV transmittance in the surface layers at Stns 1 through 5 was highly variable. Thus, K_{d305nm} decreased from 5.4 m^{-1} at Stn 1 to 2.3 m^{-1} at Stn 5 (Table 1). Due to the high attenuation, no values for K_{d305nm} could be retrieved below 1 m depth at any of the stations. The diffuse attenuation coefficients for the surface layer decreased from Stn 1 to Stn 5, also for the other wavelengths. Thus, K_{d320nm} decreased from 5.0 to 1.9 m^{-1}, K_{d340nm} decreased from 3.8 to 1.36 m^{-1}, and K_{d380nm} decreased from 2.3 to 0.76 m^{-1}. Due to higher irradiance and lower attenuation at 380 nm, significant signals could be obtained down to 10 m, so K_{d380nm} could be measured in the 7 to 10 m layer at all stations. As expected, there was a strong correlation (r = 0.90) between CDOM and K_{d380nm} (Fig. 3a). Also, the attenuation at 305 nm depended strongly on the absorption at 310 nm, and a correlation analysis was performed between K_{d305nm} and CDOM. A very high correlation with CDOM (r = 0.99) (Fig. 3b) was found, although the number of samples was small (n = 3).

The downward diffuse attenuation at 320, 340, and 380 nm was lower between 1 and 2 m than in the surface layer (0 to 1 m). At 340 and 380 nm the attenuation coefficient was found to be independent of depth below 3 m (Table 2, Fig. 4). Radiation could not be detected at 305 or 320 nm at depths below 3 m.

Profiles performed with the ac9 showed that absorption coefficients at 410 nm were independent of depth below 3 m and approximately 0.5 m^{-1} at all stations. Mean values between 7 and 10 m are shown in Table 1.

Intercomparison of downwelling diffuse attenuation coefficients retrieved from different spectroradiometers

For comparisons of diffuse attenuation coefficients retrieved simultaneously from different instruments at the same site, we used 4 different radiometers to measure downwelling UV irradiances at each station. Spectral measurements with OL754 were made at 3 depths; just below the surface (0 m) and at depths of 1 and 2 m. Spectral diffuse attenuation coefficients were estimated for the layers between 0 and 1 m, and 1 and 2 m. Two identical PUV500 were used in the campaign. Diffuse attenuation coefficients calculated

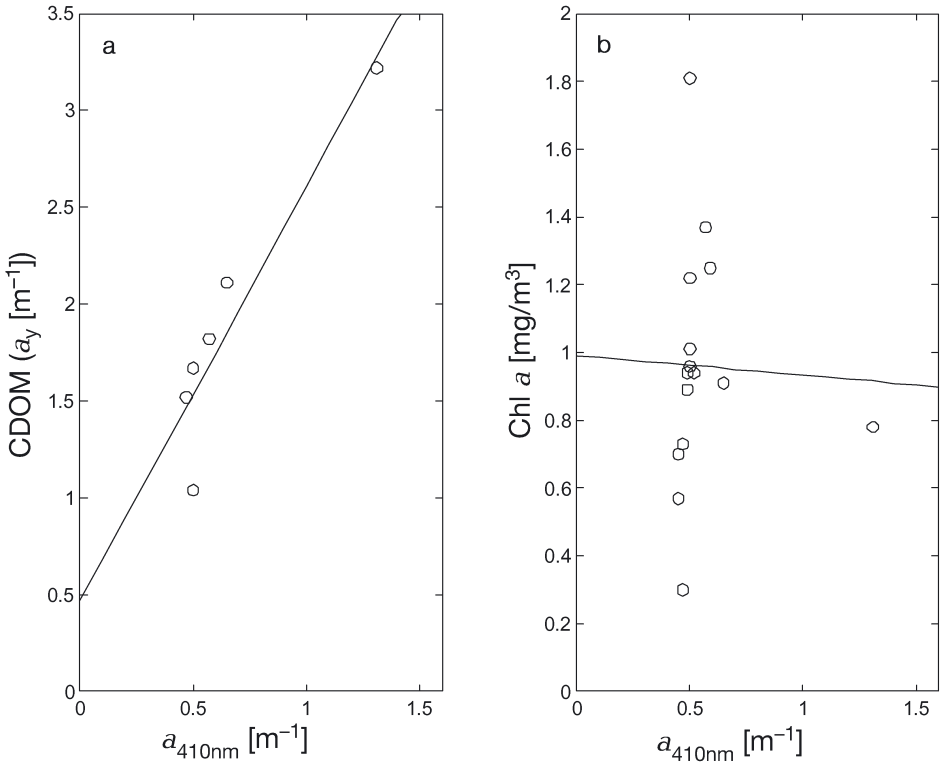

Fig. 2. (a) Correlation between colored dissolved organic matter (CDOM) (measured as absorption at 310 nm, a_y, see 'Materials and methods') and absorption coefficient a_{410nm}, measured with the profiling instrument ac9, in samples and profiling data collected at the same time and same depth. Data from Stns 1, 3 and 5 are included. (b) Correlation between chl *a* concentration and absorption coefficient a_{410nm}, measured with the profiling instrument ac9, in samples and profiling data collected at the same time and same depth. Data from Stns 1, 3 and 5 are included

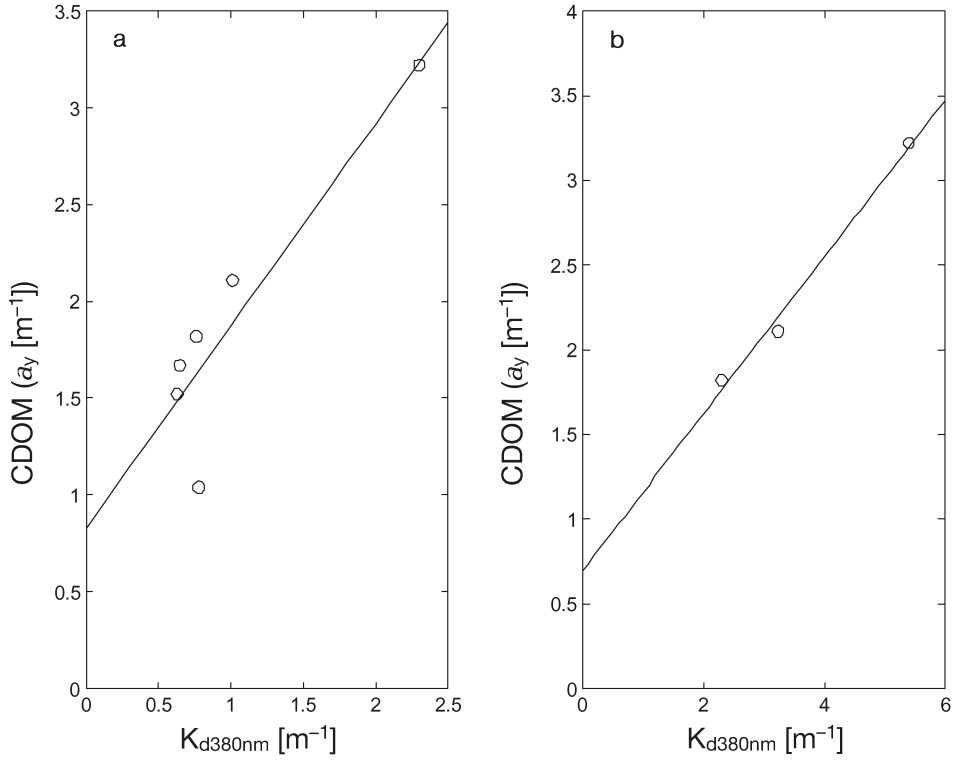

Fig. 3. (a) Correlation between colored dissolved organic matter (CDOM) (measured as absorption at 310 nm, a_y, see 'Materials and methods') and the diffuse attenuation coefficient K_{d380nm} measured with PUV500/510, measured at the same time and same depth. Data from Stns 1, 3 and 5 are included. (b) Correlation between CDOM (measured as absorption at 310 nm, a_y, see 'Materials and methods') and the diffuse attenuation coefficient K_{d305nm} measured with PUV500/510, measured at the same time and same depth. Data from Stns 1, 3 and 5 are included

Table 2. Diffuse attenuation coefficients retrieved from 3 radiometers: NA: not sufficient data; –: measurements not performed

Depth (m)	305 nm[a,b,c]	320 nm[a,b,c]	340 nm[a,b,c]	380 nm[a,b,c]
Stn 1				
0–1	3.7[a] NA[b] 5.1[c]	3.2[a] NA[b] 4.1[c]	2.3[a] 1.8[b] 3.2[c]	1.4[a] 0.85[b] 1.9[c]
1–2	2.5[a] NA[b] NA[c]	2.1[a] NA[b] 2.1[c]	1.5[a] 1.3[b] 1.6[c]	0.8[a] 0.79[b] 0.9[c]
Stn 3				
0–1	3.8[a] NA[b] 3.2[c]	3.2[a] 2.26[b] 2.9[c]	2.4[a] 1.84[b] 2.1[c]	1.3[a] 1.02[b] 1.2[c]
1–2	3.1[a] NA[b] NA[c]	2.4[a] 1.38[b] 2.1[c]	1.7[a] 1.42[b] 1.6[c]	0.9[a] 0.80[b] 1.0[c]
Stn 5				
0–1	2.2[a] NA[b] 2.6[c]	1.6[a] 1.59[b] 1.9[c]	1.0[a] 1.28[b] 1.4[c]	0.3[a] 0.48[b]0.8[c]
1–2	–[a] NA[b] 2.6[c]	–[a] 1.25[b] 1.8[c]	–[a] 1.18[b] 1.3[c]	–[a] 0.63[b]0.7[c]
Stn 6				
0–1	–[a] NA[b] 2.2[c]	–[a] 1.3[b] 1.4[c]	–[a] 1.1[b] 1.1[c]	–[a] 0.6[b]0.6[c]
1–2	–[a] NA[b] 2.0[c]	–[a] 1.4[b] 1.5[c]	–[a] 1.1[b] 1.2[c]	–[a] 0.6[b]0.6[c]

[a]OL754 Optronic spectroradiometer, bandwidth 1.0 nm
[b]SMPR; equivalent wavelength 305,4 nm, 323,3 nm, 338,2 nm, 380,3 nm
[c]PUV500 Biospherical; centre bandwidth

from data obtained with these 2 instruments were indistinguishable. Therefore, results from only one of them are shown. Table 2 summarizes K_d values obtained with data from OL754, SMPR, and PUV500 at 4 stations (Stns 1, 3, 5, and 6, see Fig. 1) for the 2 layers 0 to 1 m and 1 to 2 m.

At 305 nm the attenuation in the surface layer (0 to 1 m) was estimated using data from both OL754 and PUV500. At Stn 1 diffuse attenuation coefficients retrieved from PUV500 data were 38% higher than those retrieved from OL754 data (5.1 vs 3.7 m^{-1}, Table 2). At Stn 3 the PUV500 values were 16% lower than the OL754 values (3.2 vs 3.8 m^{-1}), and at Stn 5 they were 18% higher (2.6 vs 2.2 m^{-1}).

At 320 nm K_d values obtained with data from all 3 instruments were compared, except at Stns 1 and 6 (Table 2). For the surface layer at Stn 3, SMPR and PUV500 data gave K_d values that were respectively 29 and 9% lower than the corresponding values obtained with OL754 data, and for the 1 to 2 m layer the SMPR and PUV500 values were respectively 43 and 13% lower than the OL754 values. In the surface layer at Stn 5 the K_{d320nm} values obtained with SMPR data and OL754 data were equal, whereas the PUV500 data gave K_{d320nm} values that were 19% higher. In the surface layer at Stn 1, the K_d values derived from PUV500 data were 28% higher than those derived from OL754 data. However, for the layer between 1 and 2 m the PUV values were equal to the OL754 values. It was not possible to derive diffuse attenuation coefficients for the 320 nm channel of the SMPR at Stn 1.

For comparisons of K_d values at 340 nm, measurements from all 3 instruments were available at 3 of the stations. In the surface layer (0 to 1 m) at Stn 1, K_{d340nm} values obtained with data from SMPR and PUV500 were respectively 22% lower and 39% higher than the OL754 values. In the layer between 1 and 2 m the deviations between K_{d340nm} values were smaller. The SMPR and PUV500 values were respectively 13% lower and 7% higher than the OL754 values. At Stn 3 all instruments gave K_{d340nm} values that agreed fairly well for the layer between 1 and 2 m. Thus, the SMPR and PUV500 values were respectively 16 and 6% lower lower than the OL754 values. In the surface layer larger deviations were found between the K_{d340nm} values at this station. The SMPR and

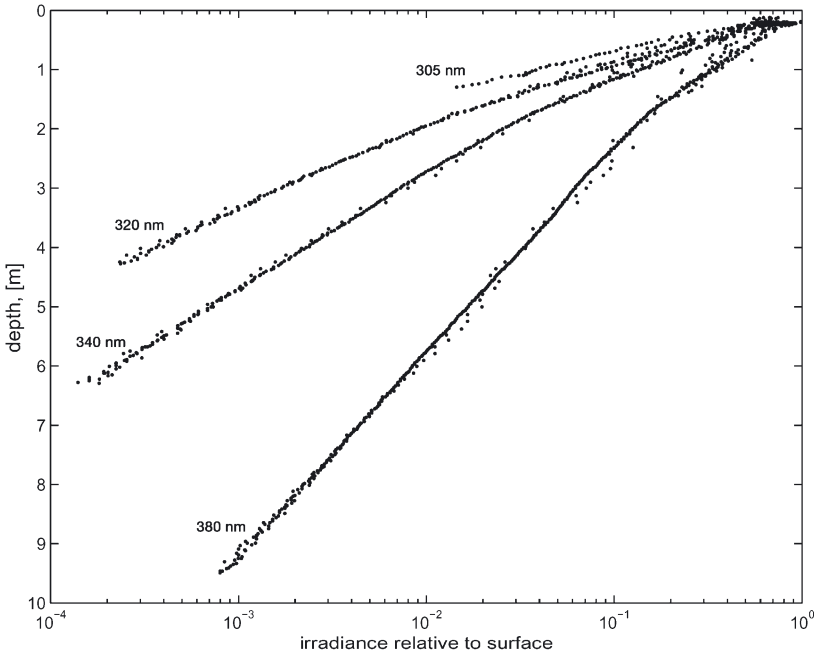

Fig. 4. Downwelling irradiance as a function of depth for 305, 320, 340, and 380 nm measured at Stn 1 with PUV500. Irradiances at different depths are relative to surface values being measured simultaneously with PUV510. Data were collected both during submerging and lifting to surface

PUV500 values were respectively 23 and 13% lower than the OL754 values. In the surface layer at Stn 5 the SMPR and PUV500 values for K_{d340nm} were respectively 28 and 40% higher than the OL754 values.

At Stn 6, only data from the profiling filter radiometer instruments (SMPR and PUV500) were available, and the K_d values agreed very well for 320, 340, and 380 nm, both in the surface layer (0 to 1 m) and in the 1 to 2 m layer.

At all wavelengths, the largest deviations between K_d values were found in the surface layer (0 to 1 m) at Stns 1 and 3 (Table 2). At both stations there was a high attenuation of UV, and the water masses were stratified. Profiles of downwelling irradiances measured at Stn 1 with the PUV500 (Fig. 4) indicated a change in the slope between 1 and 2 m. Comparisons between different instruments place high demands on the accuracy of both depth and radiation sensors. A small variability between depth sensors may have caused deviations between the K_d values obtained with data from different instruments in strongly stratified water. Salinity profiles taken at Stns 5 and 6 showed a more weakly stratified water mass than at Stn 1, and smaller deviations between K_d values were found.

An exponential dependence of K_d as a function of wavelength (λ) according to Markager & Vincent (2000) can be written as:

$$K_d(\lambda) = K_d(\lambda_0)e^{S_k(\lambda_0 - \lambda)} + K_{back}$$

Due to lack of data between 400 and 500 nm for all instruments, a good estimate of K_{back} was difficult. We assumed K_{back} to be small in this marine environment with small content of particles. Thus, in practice we used the expression suggested by Morris et al. (1995) and Laurion et al. (1997), where K_{back} is zero. S_k (coefficient that determines the shape of the curve) was found to be 0.014 nm^{-1} in the surface layer (0 to 1 m) and 0.015 nm^{-1} in the 1 to 2 m layer based on spectral measurements with OL754 at Stn 1 (Fig. 5). At Stn 3, S_k was found to be 0.015 nm^{-1} in the surface layer (0 to 1 m) and 0.016 nm^{-1} in the 1 to 2 m layer (Fig. 6). Thus, S_k might be slightly low due to the estimate of K_{back} used.

The above equation should apply also to the filter radiometer data. Deviations from the exponential dependence for data from SMPR and PUV500 could be taken as an indication of possible problems with these measurements. Interpolation between K_d values obtained from PUV500 gave a S_k value of 0.013 nm^{-1} for the surface layer at Stn 1 and 0.014 nm^{-1} for the 1 to 2 m layer (note that only 3 wavelengths were available for the 1 to 2 m layer) (Fig. 5). At Stn 3 the K_d values at 305 nm derived from PUV500 data were lower than expected (3.2 m^{-1} compared with 3.8 m^{-1} from OL754 data) (Fig. 6). Excluding the wavelength of 305 nm, we obtained a b value equal to 0.014 nm^{-1} for the surface layer (0 to 1 m) and 0.012 nm^{-1} for the 1 to 2 m layer based on PUV500 data.

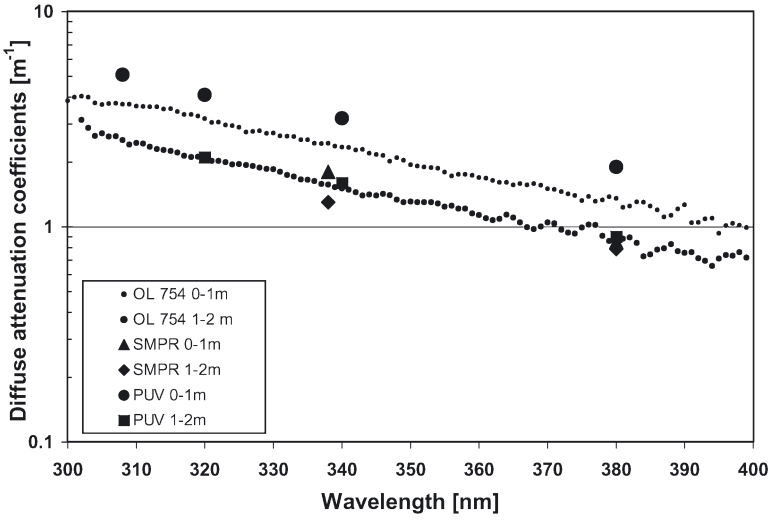

Fig. 5. Diffuse attenuation coefficients as a function of wavelength retrieved from downwelling irradiances measured at Stn 1 in the surface layer (0 to 1 m) and in the 1 to 2 m layer with the OL754 spectroradiometer, the SMPR and the PUV500 filter radiometer

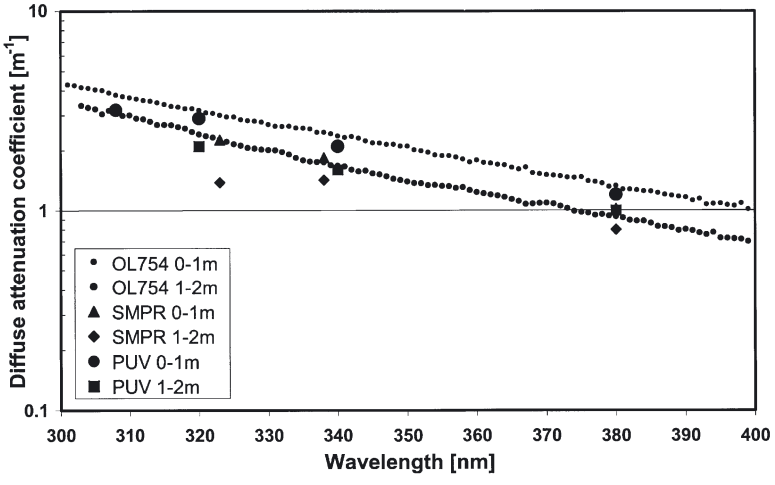

Fig. 6. Diffuse attenuation coefficients as a function of wavelength retrieved from downwelling irradiance measurements at Stn 3 in the surface layer (0 to 1 m) and in the 1 to 2 m layer with the OL754 spectroradiometer, the SMPR and the PUV500 filter radiometer

DISCUSSION

In a narrow fjord such as the Samnanger fjord, Norway, with run off from surrounding rivers, the optical properties of the water column are spatially and temporally variable and depend upon local conditions. Freshwater supplies, and tidal and/or wind generated horizontal advection, give rise to both mixed and stratified water masses. During this cruise, the innermost part of the fjord (Stn 1) had a 1 m layer of freshwater with a high concentration of humic substances, probably originating from river water and/or drainage water. Since there had been calm wind conditions prior to the cruise, no mixing had occurred, and therefore, stratified water masses were observed. Daily salinity profiles showed almost no mixing during the cruise and the low salinity surface layer prevailed for several days. The phytoplankton concentration was low in the layer between 0 and 10 m, but the amount of CDOM (proportional to the absorption at 310 nm) was high (Table 1). This resulted in very high UV absorption in the upper layer, with attenuation coefficients in the range of 3 to 5 m^{-1} at 320 nm (Tables 1 & 2). In principle, the fjord water was covered by an efficient UV filter lasting for several days. This layer could not only be observed in the inner part of the fjord, but extended outwards towards Stn 3. Correspondingly, the diffuse attenuation coefficients at 320 nm at Stn 3 were quite high, 2.3 to 3.2 m^{-1} (Tables 1 & 2, Fig. 6). However, they are lower than the values at Stn 1 due to less fresh water discharge. At Stn 5 the water masses were more mixed. CDOM and absorption at 410 nm at Stn 3 were slightly less than or comparable with what was found at Stn 5 (a_{y310} = 2.11 and 1.82 m^{-1} and a_{410} = 0.65 and 0.57 m^{-1} respectively, Table 1); the same tendency was found for the UV attenuation (K_{d320nm} values of 2.4 and 1.9 m^{-1}, Table 1). At Stn 6 UV attenuation was even lower (K_{d320nm} = 1.1 m^{-1}, Table 2). At Stn 5 there were higher chlorophyll concentrations in the surface layer than at Stns 1 and 3 (Table 1). Changes in the UV penetration associated with marine intrusions and freshwater discharge were also found in a shallow coastal lagoon of the Southern Atlantic Ocean by Conde et al. (2000). In this system K_d values in the UVB and UVA regions were higher, ranging from 7.3 to 2.1 m^{-1}, respectively. In the most turbid regions the K_d values for the UVB region ranged from 29 to 64 m^{-1} (Conde et al. 2000). The exponential coefficient S_k, ranging from 0.013 to 0.015 nm^{-1}, is within the range found in other marine systems, but in most of these analyses absorption properties, rather than diffuse attenuation coefficients, have been investigated (Markager & Vincent 2000, but aso see Belzile et al. 2002). Care should be taken when comparing S_k from different marine systems, particularly if K_{back} (see earlier equation) is not reported. For lakes, differences in S_k of up to 67% have been reported (Markager & Vincent 2000).

Comparisons of K_d values that were calculated using data from different instruments at the same stations revealed deviations as large as 40% (Table 2) in the surface layer (0 to 1 m) at Stns 1 and 3 for the shortest wavelengths (305 and 320 nm). In highly stratified water masses, such comparisons place high demands on measurement techniques. There should be a high number of repetitions per layer, and measurements by all instruments should ideally be performed at the same time (i.e. at the same solar zenith angle). Also, the methods used to measure depth are important. Both the OL754 and the PUV500 instruments were submerged just below the surface (ca. 10 to 20 cm) and were slowly lowered with a winch. The OL754 measured at specific depths that were controlled manually from the submerged cable. Irradiance measurements by the PUV500 were selected according to the depth readings of the instrument. The SMPR was submerged without a winch and was in free fall. This inhibited effective data collection in the upper 2 m of the water column. Data at different depths were selected according to the depth sensor of the instrument. Although it is difficult from this investigation to directly discern why there were such high deviations between K_d values calculated with data from different instruments, there is no doubt that small deviations between depth measurements may have resulted in different K_d values at the same station. Smaller deviations were found at Stns 5 and 6, which both had a lower UV attenuation and more mixed water masses than the 2 innermost stations (Table 5). Kirk et al. (1994) performed a similar intercomparison of K_d values calculated from spectral measurements using both an Optronic 752 and a PUV500 instrument in 2 different freshwater lakes, one being clear and the other moderately colored. In that study the instruments were fastened to a common platform, and lowered to the same depths for simultaneous measurements. There was relatively good agreement for wavelengths above 320 nm in both lakes. However, in the colored lake, there was a discrepancy for the 305 nm channel — seemingly an underestimate. Similarly, the results reported here indicate that the PUV500 underestimated the K_d value at 305 nm compared with the values at 320, 340, and 380 nm at Stn 3 (Fig. 6, 0 to 1 m layer). Similar discrepancies on performance of the PUV500 have been reported by Laurion et al. (1997). The 305 nm channel of the PUV500 has a broad bandwidth, and the spectral shape of the solar spectrum changes with depth because the short-wavelength UVB radiation is attenuated more than long-wavelength UVB radiation. This likely causes the irradiance measured by this instrument to be higher than with a narrowband instrument with a 1 nm bandwidth. As a

result, a smaller attenuation coefficient will be measured with the PUV500 instrument than with a spectral instrument or a narrow band filter instrument with bandwidth of 1 or 2 nm. Thus, measurements with the PUV500 yields lower attenuation values than those obtained from an instrument with a narrower spectral resolution (as reported by Booth et al. 1994).

SUMMARY

CDOM was found to be the most important component affecting the UV attenuation in the Samnanger fjord. The cruise revealed that there is a strong gradient in optical properties, not only vertically, but also in the horizontal direction of the fjord. There are few results published from similar systems, but it is likely that this pattern is typical for deep-silled Norwegian fjords. These findings are of great importance for the adjacent coastal water due to the exchange processes between fjord water and coastal water (Erga 1989, 1990, Frette et al. 2001).

Measurements of underwater UV penetration are challenging. Instrument intercomparisons are valuable since they reveal discrepancies caused by instrumental differences (i.e. bandwith, free-fall or controlled depth), and those that can be caused by small differences made during the measurements (e.g. changes in solar zenith angle and the depth at which measurements are made). The latter is particularly critical when the water masses are highly stratified. As has been the case with terrestrial radiometers (Bais et al. 2001), perhaps repetition of intercomparisons such as this will minimize the discrepancies currently found with underwater radiometer measurements, and the properties derived from them.

Acknowledgements. H.I.B. and P.K.'s contribution to this project was supported by the Norwegian Institute of Marine Research and by Project #140472/130 from the Research Council of Norway. We thank the crew of RV 'Hans Brattstrøm' for their kind assistance during the cruise.

LITERATURE CITED

Aas E, Høkedal J (1996) Penetration of ultraviolet B, blue and quanta irradiance into Svalbard waters. Polar Res 15: 127–138

Aas E, Højerslev NK (2001) Attenuation of ultraviolet irradiance in north European coastal waters. Oceanologia 43: 139–168

Arts MT, Robarts RD, Kasai F, Waiser MJ, Tumber VP, Plante AJ, Rai H, de Lange HJ (2000) The attenuation of ultraviolet radiation in high dissolved organic carbon waters of wetlands and alkes on the northern Great Plains. Limnol Oceanogr 45:292–299

Bais A, Gardiner BG, Slaper H, Blumthaler M and 20 others (2001) The SUSPEN intercomparison of Ultraviolet spectroradiometers. J Geophys Res D 106:12509–12525

Belzile C, Gibson JAE, Vincent WF (2002) Colored dissolved organic matter and dissolved organic carbon exclusion from lake ice: implications for irradiance transmission and carbon cycling. Limnol Oceanogr 47:1283–1293

Booth CR, Morrow JH (1997) The penetration of natural UV into natural waters. Photochem Photobiol 65:254–257

Booth CR, Mestechkina T, Morrow JH (1994) Errors in the reporting of solar spectral irradiance using a moderate bandwidth radiometer: an experimental investigation. In: Jaffe JS (ed) Ocean Optics XII Conference, Bergen, Norway, June 13–15, 1994. Proc Soc Photo-optical instrumentation Engineers (SPIE), 2258. SPIE, Bellingham, p 654–663

Browman HI, Rodriguez CA, Béland F, Cullen JJ and 7 others (2000) Impact of ultraviolet radiation on marine crustacean zooplankton and ichthyoplankton: a synthesis of results from the estuary and Gulf of St.Lawrence, Canada. Mar Ecol Prog Ser 199:293–311

Conde D, Aubriot L, Sommaruga R (2000) Changes in UV penetration associated with marine intrusions and freshwater discharge in a shallow coastal lagoon of the Southern Atlantic Ocean. Mar Ecol Prog Ser 207:19–31

Crump D, Lean D, Berrill M, Coulson D, Toy L (1999) Spectral irradiance in pond water: influence of water chemistry. Photochem Photobiol 70:893–901

DeMora S, Demers S, Vernet M (2000) The effects of UV radiation in the marine environment. Cambridge University Press, Cambridge

Dunne RP, Brown BE (1996) Penetration of solar UVB radiation in shallow tropical waters and its potential biological effects on coral reefs: results from the central Indian Ocean and Andaman Sea. Mar Ecol Prog Ser 144:109–118

Erga SR (1989) Ecological studies on the phytoplankton of Boknafjorden, Western Norway. 1. The effect of water exchange processes and environmental factors on temporal and vertical variability of biomass. Sarsia 74:161–176

Erga SR (1990) The importance of external physical controls on vertical distribution of phytoplankton and primary production in fjords of Western Norway. PhD thesis, University of Bergen

Frette Ø, Erga SR, Stamnes JJ, Stamnes K (2001) Optical remote sensing of waters with vertical structure. Appl Opt 40:1478–1487

Gunn JM, Snucins E, Yan ND, Arts MT (2001) Use of water clarity to monitor the effects of climate change and other stressors on oligotrophic lakes. Environ Monit Assess 67: 69–88

Hessen DO (2001) UV radiation and Arctic ecosystems. Springer, Berlin

Højerslev NK, Aas E (1998) Spectral light absorption by yellow substance in the Kattegat-Skagerrak area. Oceanologia 43:39–60

Holm-Hansen O, Lorentzen CJ, Holmes RW, Strickland JDH (1965) Fluorometric determination of chlorophyll. J Cons 30:3–15

Kirk JTO, Hargreaves DP, Morris DP, Coffin RB and 9 others (1994) Measurements of UV-B radiation in two freshwater lakes: an instrument intercomparison. Arch Microbiol 43: 71–99

Kjeldstad B, Johnsson B, Koskela T (1997) The Nordic intercomparison of ultraviolet and total ozone instruments at Izana, October 1996. Finnish Meteorological Institute, Meteorological Publications No. 36, Helsinki

Kuhn P, Browman HI, McArthur B, St-Pierre JF (1999) Penetration of ultraviolet radiation in the waters of the estuary and Gulf of St. Lawence. Limnol Oceanogr 44:710–716

Laurion I, Vincent WF, Lean DRS (1997) Underwater ultraviolet radiation: development of spectral models for northern high latitude lakes. Photochem Photobiol 65:107–114

Leszczynski K, Jokela K, Ylianttila L, Visuri R, Blumthaler M (1998) Erythemally weighted radiometers in solar UV monitoring: results from the WMO/STUK intercomparison Photochem Photobiol 67:212–221

Markager S, Vincent WF (2000) Spectra light attenuation and the absorption of UV and blue light in natural waters. Limnol Oceanogr 45:642–650

Morris DP, Zagarese HE, Williamson CE, Balseiro EG, Hargreaves BR, Modenutti B, Moeller R, Oueimalinos C (1995) The attenuation of solar UV radiation in lakes and the role of dissolved organic carbon. Limnol Oceanogr 40: 1381–1391

Piazena H, Häder DP (1994) Penetration of solar UV irradiation in coastal lagoons of the southern Baltic Sea and its effect on phytoplankton communities. Photochem Photobiol 60:463–469

Scully NM, Lean DRS (1994) The attenuation of ultraviolet radiation in temperate lakes. Arch Hydrobiol 43:135–144

Webb A (1997) Advances in solar ultraviolet spectroradiometry. Air Pollution Research Report 63, European Commission, Brussels

Editorial responsibility: Otto Kinne (Editor), Oldendorf/Luhe, Germany

Submitted: May 10, 2002; Accepted: March 15, 2003
Proofs received from author(s): June 20, 2003